

RESEARCH ARTICLE

PL-GAN: Path Loss Prediction Using Generative Adversarial Networks

AHMED MAREY, MUSTAFA BAL^{ID}, HASAN F. ATES^{ID}, (Senior Member, IEEE),
AND BAHADIR K. GUNTURK^{ID}

School of Engineering and Natural Sciences, Istanbul Medipol University, 34810 Istanbul, Turkey

Corresponding author: Bahadir K. Gunturk (bkgunturk@medipol.edu.tr)

This work was supported by The Scientific and Technological Research Council of Turkey (TUBITAK) Grant 215E324.

ABSTRACT Accurate prediction of path loss is essential for the design and optimization of wireless communication networks. Existing path loss prediction methods typically suffer from the trade-off between accuracy and computational efficiency. In this paper, we present a deep learning based approach with clear advantages over the existing ones. The proposed method is based on the Generative Adversarial Network (GAN) technique to predict path loss map of a target area from the satellite image or the height map of the area. The proposed method produces the path loss map of the entire target area in a single inference, with accuracy close to the one produced by ray tracing simulations. The method is tested at 900MHz transmission frequency; the trained model and source codes are publicly available on a Github page.

INDEX TERMS Deep learning, height maps, satellite images, GANS, channel parameter estimation, wireless network, regression, excess path loss, air-to-ground communication system.

I. INTRODUCTION

Path loss, which refers to the signal power reduction between transmitter and receiver antennas, is a critical component in the design and optimization of wireless communication networks. Path loss is affected by many factors, including the reflection, refraction and absorption of electromagnetic waves, terrain, vegetation, and weather conditions. Simple analytical models, such as the free-space model and the two-ray ground reflection model, are insufficient for urban environments and irregular terrains. There are empirical models (e.g., Okumura-Hata [1], [2] and COST Hata [3]) that are aimed for urban environments; these models require a characterization of the environment as, for example, “sub-urban”, “urban” and “metropolitan” [4]; however, such a general classification may not reflect the actual characteristics of a specific area or a specific transmitter-receiver path. Various models have been developed to incorporate the local features along the transmitter-receiver path. For instance, Walfisch-Ikegami model [3] includes parameters, such as average building heights, average road widths and

road orientation between transmitter and receiver. There are also alternative parametric models, such as the alpha-beta-gamma and the close-in models [5], which do not define the parameter values based on specific building characteristics but require the optimization of parameters from measurement data.

Compared to analytical and empirical models, ray tracing simulations result in more accurate predictions in urban environments when there is a 3D model of the region [6], [7], [8]. The downside of ray tracing simulations is the high computational cost, making it impractical for network planning applications.

Machine learning based approaches have also been utilized for path loss prediction. Traditional machine learning methods use hand-crafted features (e.g., building density, average building height and average street width) to train a model [9], [10]. The training data may be obtained from ray tracing simulations or field measurements.

The need for choosing the right features is a major issue in traditional machine learning methods; deep learning methods overcome this issue by learning the features as well during the training process. In recent years, deep learning based path loss prediction methods have been proposed. In [11],

The associate editor coordinating the review of this manuscript and approving it for publication was Razi Iqbal^{ID}.

the satellite image of a target area is input to a convolutional neural network (CNN) to produce path loss model parameters. The path loss model is the log-distance path model; the network predicts the path loss exponent and shadowing factor of the model. In [12], the path loss distribution of an area, instead of specific model parameters, is predicted again from satellite images. The path loss distribution does not tell the path loss value at a specific point, but it can be used to determine critical regional values, such as the coverage area. In [13], the building profile between transmitter and receiver is input to a deep fully connected neural network to predict the path loss value at the receiver. The main disadvantage of such point-to-point path loss modeling is the need to run the network for each receiver point. There are also methods that combine features extracted from satellite images with some additional features (e.g. transmitter height, receiver height, transmitter-receiver distance and frequency), and then input to a neural network for path loss regression [14], [15].

In this paper, we present a deep learning based approach to predict path loss at every point in a target region (in a single inference) directly from the satellite image or the height map of the region. This is a clear advantage over the point-to-point prediction models, which require a separate inference for each point, and over the parametric prediction models, which fit a global model for the entire region and do not predict path loss at every receiver point.

Our approach is based on the Generator Adversarial Network (GAN) technique. GANs are typically used in computer vision for style transfer applications [16]. We are able to adopt the GAN technique by treating path loss values of the target region as an image. The proposed network, which we call PL-GAN, is trained with data obtained from extensive ray tracing simulations. The trained network produces path loss values almost instantly, with accuracy close to ray tracing simulations. The trained model and source codes are publicly available on a Github page¹.

The paper is organized as follows. In Section II, we describe how the training/testing dataset is generated. We present the proposed network architecture in Section III. We explain the training method in Section IV. We present the results in Section V and conclude the paper in Section VI.²

II. DATASET GENERATION

The dataset is generated following the process described in [11] and [12] with some changes necessary for the proposed architecture. We have the satellite images and corresponding 3D models of some urban/suburban regions, each with size $1.8\text{km} \times 1.8\text{km}$ [11]. The PlaceMaker³ extension for Google SketchUp⁴ is used to obtain the 3D models along with the satellite images. The 3D models are imported and merged with a flat terrain in Wireless InSite⁵ ray tracing simulation

environment. The terrain is set as dry earth and the building material is set as concrete. In each model, the transmitter is placed at the center of a region at a height of 40m above ground. The receivers are placed at 1.5m above ground on a 110×110 grid. The transmitter power is set to 60 dBm, the transmission frequency is set to 900 MHz, and the antenna type is set as an omni-directional antenna. Using the ray tracing simulations, excess path loss values at the receivers are calculated. (Receivers that are placed inside the buildings are known since the 3D models are available. The path loss values corresponding to these locations are not reliable, and they are excluded from the final performance evaluation, as we will explain later.)

The size of each satellite image is 256×256 ; to match this size, the path loss values on the 110×110 grid is resized to 256×256 with bilinear interpolation.

As an alternative to satellite images, we want to investigate the use of 3D models to predict path loss values. 3D models are converted to height map images using orthographic projection; a pixel value in a height map represents the height of that point in the 3D model. The height maps are also resized to 256×256 to match the sizes of satellite images and path loss images.

A block diagram of the dataset generation process is presented in Figure 1. The satellite image, height map image, and path loss image of a sample region is given in Figure 2.

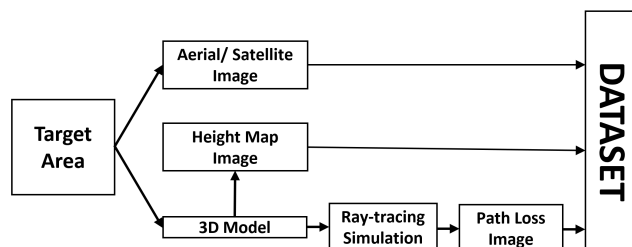


FIGURE 1. Block diagram of dataset generation. The satellite image, height map image and path loss image of each target region is added to the dataset.

III. NETWORK ARCHITECTURE

We treat path loss values on a grid of receivers as an image; this allows us to utilize image synthesis methods in the path loss prediction. Generative Adversarial Network (GAN) is a recently developed deep learning based image synthesis approach; it has been successfully used in style transfer, inpainting, super resolution and image-to-image translation. GAN training includes two networks: a generator network to generate new examples, and a discriminator network to classify examples as real or fake [16].

Our idea is to use GAN to produce path loss image (that is, path loss values on a grid of receivers in the entire target region) from a satellite or a height map image. The proposed generator and discriminator architectures are presented in Figures 3 and 4, respectively. The generator is essentially a U-Net structure with skip connections, which is known to allow deeper architectures. We use 15 convolutional blocks

²<https://github.com/ahmarey/PLGAN>

³<https://www.supacemaker.com>

⁴<https://www.sketchup.com>

⁵<https://www.remcom.com/wireless-insite-em-propagation-software>

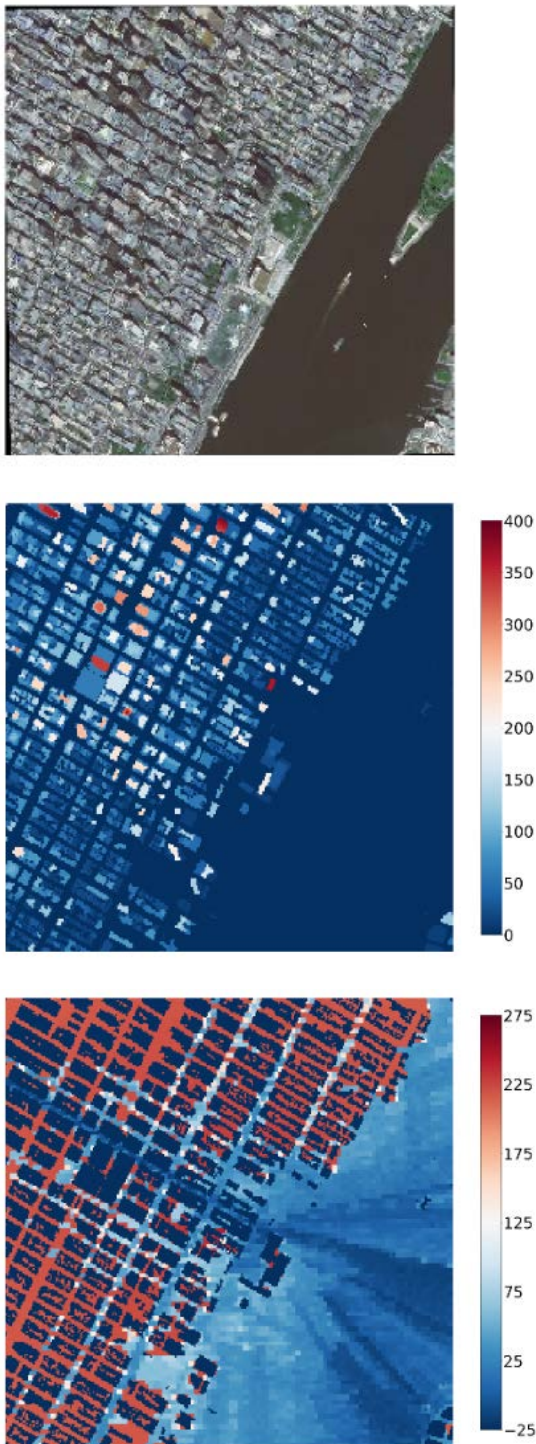


FIGURE 2. Satellite image, height map image and path loss image (in order from top to bottom) of a sample region. For the height map image, the color bar indicates height in meters. For the path loss image, the color bar indicates the excess path loss in dB; pixels corresponding to receivers inside buildings are marked with -25dB , which is a random choice that is smaller than all actual excess path loss measurements, for visualization purposes.

in a conventional encoder-decoder structure, first, decreasing the size (height and width) while increasing the depth (number of channels), followed by transpose convolutions to

increase the size while reducing the depth until the original image dimensions are reached. (The generator architecture is given in Figure 3.)

For the discriminator, we use a patch discriminator [17] that decides on each patch of the generator output as true or fake. The advantage of patch discriminator is that it has fewer parameters, can be applied to arbitrarily large images, and has been shown to produce high quality results [18]. We use stride of two at the initial layers to reduce the number of parameters to be estimated while preferring stride of one later in order not to lose the image details. The discriminator has the concatenation of generated image and true image as its input; and it consists of eight convolutional blocks, producing an output of size $5 \times 5 \times 1$ for each patch. (The discriminator architecture is given in Figure 4.)

The loss functions and the training process are described in the next section. Regarding the architectures, we tried some other variations as well. Using a small sized output for the discriminator and having enough depth turned out to be crucial for the current success.

IV. TRAINING THE NETWORKS

We train two separate networks, one for satellite image as the input and one for height map as the input. At the end, we will compare their performances. The training process is very similar for both cases, except for some minor changes. Training a GAN network is not straightforward; in this section, we explain our training process in detail. The final goal of GAN training is such that the generator is able to deceive a well-trained discriminator.

The loss function for the generator training has two components, as illustrated in Figure 5. One loss component measures how well the discriminator is deceived. An input image, which is either a satellite image or a height map, is passed to the generator. The generated path loss image is input to the discriminator, which decides patch-by-patch whether the generator output is true. The discriminator output is compared against an array of ones, each corresponding to patch; and binary cross entropy is used as the cost function. In the perfect case, the discriminator is totally deceived and produces an output of one for each patch. The other loss component is the L1 loss between the true path loss image and the generated path loss image. Finally, a weighted sum of the binary cross-entropy loss and L1 loss is taken, where the weight of the L1 loss is 100 times the other weight, as suggested in [18].

The generator training is modified slightly for the height map network. When the input image is satellite image, the L1 loss between the generated and true images is calculated for all pixels. When the input image height map, we know whether a pixel corresponds to an indoor location or an outdoor location. Therefore, the L1 loss is calculated for only the outdoor pixels, forcing the network to minimize the error on the outdoor path loss estimation and disregard the error for the indoor locations.

For the discriminator, the goal is to train a network that distinguishes between true and fake path loss images.

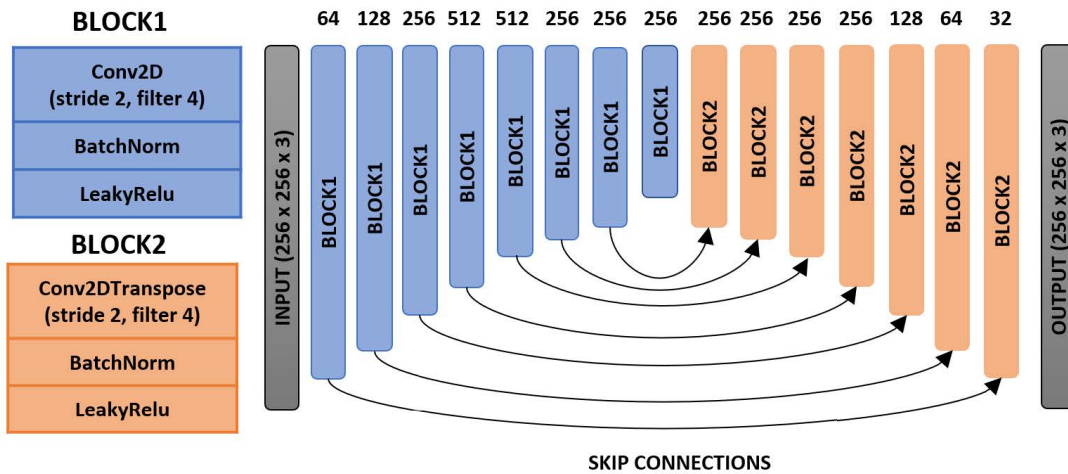


FIGURE 3. The generator architecture. BLOCK1, which consists of 2D convolution with filter size 4×4 and stride 2, batch normalization and Leaky ReLU layers, is repeated eight times. These layers are followed by upsampling layers. The upsampling layers include repeated application of BLOCK2, which consists of transpose convolution with filter size 4×4 and stride 2, batch normalization and Leaky ReLU layers. The number of filters is indicated above each block.

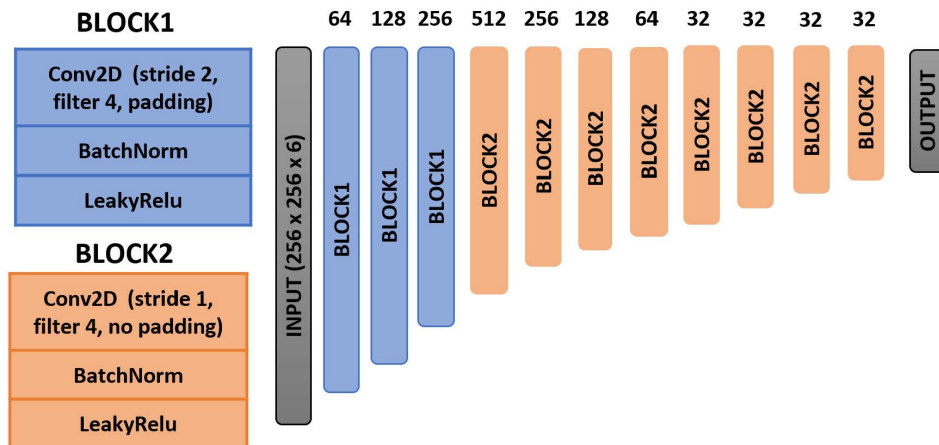


FIGURE 4. The discriminator architecture. BLOCK1, which consists of 2D convolution with filter size 4×4 and stride 2, batch normalization and Leaky ReLU layers, is repeated three times. These layers are followed by repeated application of BLOCK2, which consists of 2D convolution with filter size 4×4 and with stride 1, batch normalization and Leaky ReLU layers. The number of filters is indicated above each block.

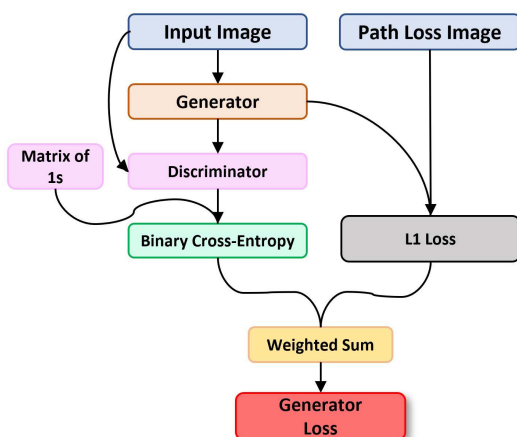


FIGURE 5. The loss function for the generator training.

The discriminator takes two inputs, one is the true path loss image and the other is either the generated generated path

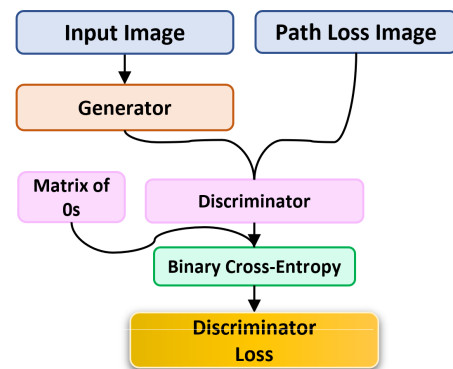


FIGURE 6. The loss function for the discriminator training when true and generated images are input.

loss image or the true path loss image. When the inputs are true path loss image and the generated path loss image, the discriminator should classify each patch as fake (i.e. return “0”); therefore, the loss function is binary cross-entropy loss

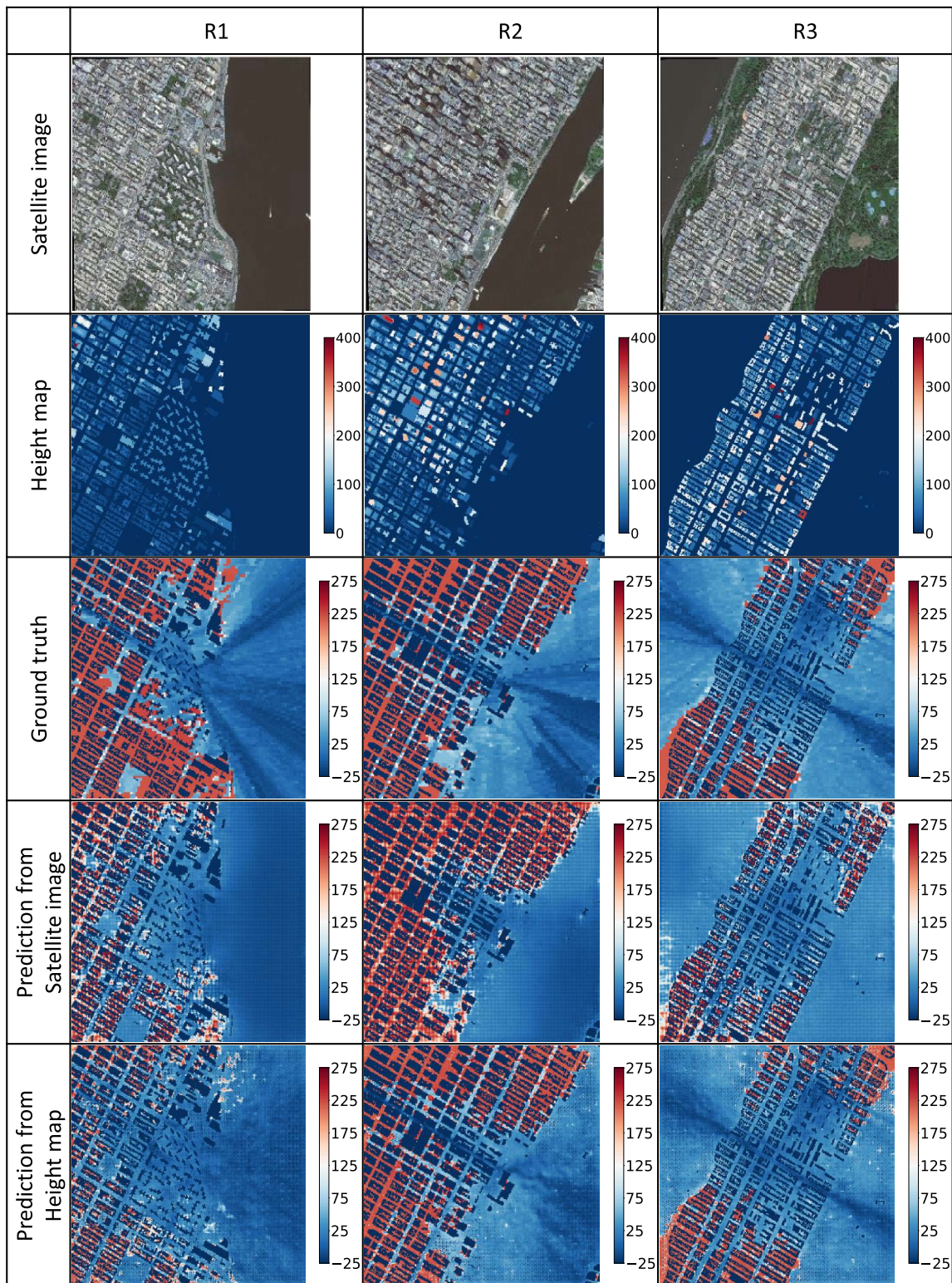


FIGURE 7. Comparison between the predicted path loss images and true path loss images for the three sample regions.

between the discriminator output and a matrix of zeros, as illustrated in Figure 6. When both input images are real path loss images, binary cross-entropy between the discriminator outputs and a matrix of ones is calculated.

The dataset, which consists of 997 image pairs, is split into training (902) and testing (95) sets. The training images are augmented, using rotations (90 and 180 degrees) and flipping (horizontal and vertical), to increase the training set size eight

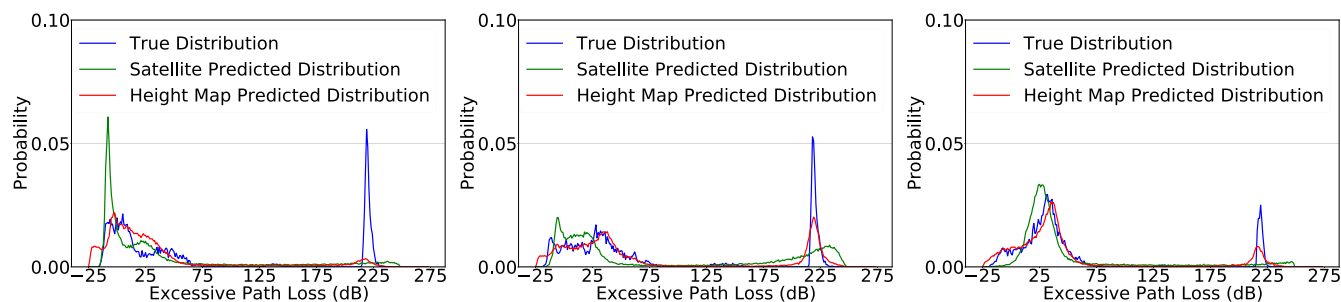


FIGURE 8. Comparison between the true distributions and the distributions obtained from predicted path loss images for the regions given in Figure 7.

TABLE 1. Evaluation of the trained networks for different input types.

	Satellite image	Height map image
Average RMSE	43.3	44.1
Average MSE between dist.	2.6×10^{-5}	4.6×10^{-5}
Average MSE between dist. [12]	160×10^{-5}	-

folds to 7216. We used Adam optimizer for training both the generator and discriminator with learning rate 0.0001 and batch size of 32. We trained the network on Tensorflow 2.0 on Nvidia RTX 2060 GPU where the training goes for about 12 hours for 500 epochs. (The trained model is available on the Github link, as mentioned before.)

V. EVALUATION

To evaluate the performance of the proposed approach, we use two quantitative measures. The first one is the root mean squared error (RMSE) between true path loss values and predicted path loss values, averaged over the entire test set. The second one is the mean squared error (MSE) between the true path loss distribution and the distribution obtained from the predicted path loss image, averaged over the entire test set.

The results are given in Table 1. The average RMSEs for satellite image and height map as input are similar. The average MSE between the distributions for satellite image as input is lower than that for height map image as input. In the table, we also included a result from [12] (the closest experiment to our scenario with satellite image as input, 900Mhz frequency, 80m altitude, eight bin representation of distribution), as a rough comparison. The average MSE results in this paper are about two folds better than the ones in [12]. The average RMSE results are about 44dB, which is satisfactory considering the fact that the dynamic range of excess path loss in the experiments is more than 270dB. In addition, the visual results indicate that path loss values including shadowing due to buildings are predicted well.

In Figure 7, we provide results for three sample regions. In the figure, the first row shows the satellite images and the second row shows the height map images. The colorbar next to the height map images indicates heights in meters. The third row shows the true excess path loss values. The color bar next to the images are the path loss values in dB. The fourth and fifth rows show the predicted excess path loss images for the network that takes satellite images as input and the network that takes height map images as input, respectively.

In these images, we note that shadowing due to buildings are captured well with both methods, while height map images can result in sharper shadowing boundaries.

In Figure 8, we show the path loss distributions for the regions given Figure 7. These results also indicate that the overall shape of the distribution can be predicted well.

VI. CONCLUSION

In this work, we present a deep learning based approach to predict the point-wise path loss values of an entire region from either height map images or satellite images. Treating path loss values of a region as an image, we use a GAN model for the supervised estimation problem. The networks can produce real-time inference and prove to be viable alternative to ray tracing simulations, which have high computational complexity.

Comparing height map images and satellite images as input, we found that height images can lead to better results. This is mainly due to the fact that definite height structure is more informative about the shadowing effects compared to satellite images.

By increasing the dataset size, it is possible to achieve better results. We leave this as a future work because other than the dataset that we have there are no public datasets that have path loss images as well as corresponding satellite images and height maps. We hope that this work will initiate further research and innovations in this area.

REFERENCES

- [1] Y. Okumura, E. Ohmori, T. Kawano, and K. Fukuda, "Field strength variability in VHF and UHF land mobile service," *Rev. Electr. Commun. Lab.*, vol. 16, nos. 9–10, pp. 825–873, 1968.
- [2] M. Hatay, "Empirical formula for propagation loss in land mobile radio services," *IEEE Trans. Veh. Technol.*, vol. VT-29, no. 3, pp. 317–325, Aug. 1980.
- [3] D. J. Cichon and T. Kürner, "Propagation prediction models," Eur. Commission, Directorate-Gen. Inf. Soc. Media, Brussels, Belgium, COST Action 231, Digit. Mobile Radio Towards Future Gener. Syst., Final Rep., 1999, pp. 115–207. Accessed: Aug. 26, 2022. [Online]. Available: <https://op.europa.eu/en/publication-detail/-/publication/f2f42003-4028-4496-af95-beaa38fd475f>
- [4] Y. Singh, "Comparison of Okumura, Hata and COST-231 models on the basis of path loss and signal strength," *Int. J. Comput. Appl.*, vol. 59, no. 11, pp. 37–41, Dec. 2012.
- [5] S. Sun, T. S. Rappaport, T. A. Thomas, A. Ghosh, H. C. Nguyen, I. Z. Kovacs, I. Rodriguez, O. Koymen, and A. Partyka, "Investigation of prediction accuracy, sensitivity, and parameter stability of large-scale propagation path loss models for 5G wireless communications," *IEEE Trans. Veh. Technol.*, vol. 65, no. 5, pp. 2843–2860, May 2016.

- [6] M. F. Iskander and Z. Yun, "Propagation prediction models for wireless communication systems," *IEEE Trans. Microw. Theory Techn.*, vol. 50, no. 3, pp. 662–673, Mar. 2002.
- [7] P. Mededović, M. Veletić, and Ž. Blagojević, "Wireless insite software verification via analysis and comparison of simulation and measurement results," in *Proc. 35th Int. Conv. (MIPRO)*, 2012, pp. 776–781.
- [8] T. K. Geok, F. Hossain, M. N. Kamaruddin, N. Z. A. Rahman, S. Thiagarajah, A. T. W. Chiat, J. Hossen, and C. P. Liew, "A comprehensive review of efficient ray-tracing techniques for wireless communication," *Int. J. Commun. Antenna Propag.*, vol. 8, no. 2, pp. 123–136, 2018.
- [9] G. Yang, Y. Zhang, Z. He, J. Wen, Z. Ji, and Y. Li, "Machine-learning-based prediction methods for path loss and delay spread in air-to-ground millimetre-wave channels," *IET Microw., Antennas Propag.*, vol. 13, no. 8, pp. 1113–1121, Jul. 2019.
- [10] Y. Zhang, J. Wen, G. Yang, Z. He, and J. Wang, "Path loss prediction based on machine learning: Principle, method, and data expansion," *Appl. Sci.*, vol. 9, no. 9, p. 1908, 2019.
- [11] H. F. Ates, S. M. Hashir, T. Baykas, and B. K. Gunturk, "Path loss exponent and shadowing factor prediction from satellite images using deep learning," *IEEE Access*, vol. 7, pp. 101366–101375, 2019.
- [12] O. Ahmadien, H. F. Ates, T. Baykas, and B. K. Gunturk, "Predicting path loss distribution of an area from satellite images using deep learning," *IEEE Access*, vol. 8, pp. 64982–64991, 2020.
- [13] R.-T. Juang, "Explainable deep-learning-based path loss prediction from path profiles in urban environments," *Appl. Sci.*, vol. 11, no. 15, p. 6690, Jul. 2021. [Online]. Available: <https://www.mdpi.com/2076-3417/11/15/6690>
- [14] J. Thrane, D. Zibar, and H. L. Christiansen, "Model-aided deep learning method for path loss prediction in mobile communication systems at 2.6 GHz," *IEEE Access*, vol. 8, pp. 7925–7936, 2020.
- [15] U. S. Sani, D. T. C. Lai, and O. A. Malik, "A hybrid combination of a convolutional neural network with a regression model for path loss prediction using tiles of 2D satellite images," in *Proc. 8th Int. Conf. Intell. Adv. Syst. (ICIAS)*, Jul. 2021, pp. 1–6.
- [16] J.-Y. Zhu, T. Park, P. Isola, and A. A. Efros, "Unpaired image-to-image translation using cycle-consistent adversarial networks," in *Proc. IEEE Int. Conf. Comput. Vis.*, Oct. 2017, pp. 2223–2232.
- [17] C. Li and M. Wand, "Precomputed real-time texture synthesis with Markovian generative adversarial networks," in *Proc. Eur. Conf. Comput. Vis.* Cham, Switzerland: Springer, 2016, pp. 702–716.
- [18] P. Isola, J.-Y. Zhu, T. Zhou, and A. A. Efros, "Image-to-image translation with conditional adversarial networks," in *Proc. IEEE Conf. Comput. Vis. Pattern Recognit. (CVPR)*, Jul. 2017, pp. 1125–1134.



AHMED MAREY received the B.Sc. degree in communications and electronics engineering from the Faculty of Engineering, Alexandria University, Egypt, and the M.Sc. degree from the Department of Electrical Engineering and Cyber Systems, Istanbul Medipol University, Istanbul, Turkey, where he is currently pursuing the Ph.D. degree with the Computer Vision and Deep Learning Research Group. His current research interests include deep learning, machine learning, computer vision, signal processing, image processing, and wireless communications.



MUSTAFA BAL received the B.Sc. degree in electrical and electrical engineering from the Faculty of Engineering, İstanbul Şehir University, Turkey, in 2017, and the M.Sc. degree from the Department of Electrical Engineering and Cyber Systems, Istanbul Medipol University, Istanbul, Turkey, in 2021, where he is currently pursuing the Ph.D. degree with the Computer Vision and Deep Learning Research Group. His current research interests include deep learning, machine learning, computer vision, signal processing, image processing, and wireless communications.



HASAN F. ATES (Senior Member, IEEE) received the Ph.D. degree from the Department of Electrical Engineering, Princeton University, in 2004. He was a Research Associate at Sabanci University, from 2004 to 2005. He held positions of an Assistant, an Associate, and a Full Professorship at Isik University, from 2005 to 2018. He is currently a Professor with the Department of Computer Engineering, Istanbul Medipol University, where he joined in September 2018. He is the author/coauthor of more than 50 peer-reviewed publications in the areas of image/video processing/coding and computer vision.



BAHADIR K. GUNTURK received the B.S. degree in electrical engineering from Bilkent University, Turkey, in 1999, and the Ph.D. degree in electrical engineering from the Georgia Institute of Technology, in 2003. From 2003 to 2014, he has been with the Department of Electrical and Computer Engineering, Louisiana State University. Since 2014, he has been with Istanbul Medipol University, where he is currently a Professor. He has published more than 50 peer-reviewed journals/conference papers in the areas of image processing and computer vision.

...